DEVELOPMENT OF A PROXY-BASED VS30 MODEL FOR THE SOUTHEASTERN SOFIA BASIN – FIRST RESULTS

Lyubka Pashova, Emil Oynakov, Radan Ivanov

Assoc. Prof. Dr. Eng. Lyubka Pashova
National Institute of Geophysics, Geodesy and Geography - Bulgarian Academy of Sciences
Acad. Georgi Bonchev Str., Block 3, 1113 Sofia, Bulgaria
Tel. +359 2 979 22 73, Email: lpashova@geophys.bas.bg

Assoc. Prof. Dr. Emil Oynakov
National Institute of Geophysics, Geodesy and Geography - Bulgarian Academy of Sciences
Acad. G. Bonchev Str., Block 3, 1113 Sofia, Bulgaria
Tel. +359 2 979 37 35, Email: emil.ilievmg@gmail.com

Prof. Dr. Eng. Radan Ivanov
National Institute of Geophysics, Geodesy and Geography - Bulgarian Academy of Sciences
Acad. G. Bonchev Str., Block 3, 1113 Sofia, Bulgaria
Tel. +359 2 979 33 12; Elmail: rivanov@geophys.bas.bg

Abstract
This study presents a preliminary geologically constrained framework for developing a high-resolution hybrid Vs30 proxy map of the southeastern Sofia Basin, crucial for seismic hazard assessment and building codes. The approach integrates topographic metrics from a 100-meter DEM, lithological information from 68 boreholes, and single-station microseismic noise recordings processed using the Horizontal-to-Vertical Spectral Ratio (HVSR) method. The preliminary results indicate that local borehole and HVSR constraints can reveal near-surface heterogeneity and soft-soil zones that the global slope-based Vs30 model does not resolve. The derived Vs30 values should be interpreted as constrained estimates rather than direct measurements, because single-station HVSR inversion is non-unique and sensitive to the assumed velocity parameterization. Comparisons with existing Vs30 maps show that the new Vs30 model offers better detail and spatial precision. Based on the results, directions for future work to complete lithofacies digitization, apply regression and residual kriging, quantify uncertainties, and validate the model against independent geophysical and geotechnical datasets have been defined. Subsequent steps include incorporating multi-station microtremor arrays to constrain shallow shear-wave variations, extending ambient-noise measurements to the western Sofia Basin, and synthesizing all data into a definitive, basin-wide microzonation model to support more reliable earthquake site-amplification assessments.

Keywords: *Vs30 value, Shear-wave velocity, Proxy-based map, Topographic slope, Microtremor array, Sofia Basin*

INTRODUCTION

The averaged shear-wave velocity in the upper 30 m of the subsurface (Vs30) is widely used as a standardized proxy for near-surface sediment stiffness. It is fundamental for estimating ground-motion amplification in seismic hazard assessment, informing building code provisions, and ensuring consistent seismic site classification. Although Bulgaria does not yet have an official national Vs30 map, ongoing local mapping efforts provide an initial framework that can be further enhanced with greater methodological rigor and transparency to better support seismic hazard analyses.

Vs30 can be determined most accurately using direct borehole measurements, but non-invasive surface-wave and microtremor-array methods provide cost-effective and reliable alternatives, with geostatistical approaches useful in data-scarce regions. Several methods are used to determine Vs30: direct, surface-wave, microtremor-array, correlation-based, geostatistical, and terrain-based. Determining Vs30 involves a choice between highly accurate but expensive direct borehole methods, such as downhole or crosshole testing, and more cost-effective, non-invasive alternatives. Surface wave techniques such as spectral analysis of surface waves and microtremor array methods provide efficient means to estimate velocity profiles by analyzing seismic wave dispersion, making them ideal when drilling is impractical. For shallow or data-limited sites, correlation-based methods can safely extrapolate deeper velocities, while regional

geostatistical models and terrain proxies leverage spatial data to provide preliminary site classifications and manage uncertainty. Selecting a method requires balancing the high accuracy and cost of direct measurements with more economical surface-wave alternatives. This choice must account for site-specific conditions, such as noise and sparse data, while ensuring strict compliance with national building codes.

The Global Hybrid Vs30 model by Heath et al. (2020) provides the most recent, harmonized 30-arc-second (~1 km) grid covering Europe and Bulgaria, accessible via the USGS Earthquake Hazards Program (https://earthquake.usgs.gov/data/vs30/). The global model incorporates regional Vs30 maps for several European countries, including Italy and Greece, via weighted blending. While the model lacks a dedicated Bulgarian map, it fully covers the region using a validated slope-based proxy, serving as the primary resource for regional seismic hazard assessment until country-specific data emerges. The methodology behind the map relies on topographic slope as a proxy for near-surface shear-wave velocity, a technique validated in multiple studies and widely used for large-scale hazard modeling. Overall, the Global Hybrid Vs30 model remains the most comprehensive and up-to-date Vs30 resource for Europe and Bulgaria, pending the development of future country-specific datasets.

At the national level, several regional and urban-scale Vs30 maps have been developed using different methodologies, datasets, classification schemes, and spatial resolutions (e.g., Dineva et al., 2008; Georgieva et al., 2020). Consequently, the resulting distributions of site classes and estimated Vs30 values are not directly comparable and exhibit notable differences. Following the methodology proposed by Georgieva et al. (2020), Vs30 values were determined for several large Bulgarian cities, including Sofia, Plovdiv, and Varna. Pashova et al. (2024) emphasized the critical need for a comprehensive and high-resolution Vs30 map of Sofia, highlighting the importance of this parameter for characterizing site conditions, assessing soil dynamic behavior, and evaluating seismic ground motion. The study further underscored the necessity of detailed geophysical investigations and additional subsurface data to improve the reliability and spatial resolution of Vs30 mapping, which is essential for seismic microzonation and informed urban planning in the capital.

Another important use of Vs30 is for classifying soil type according to Eurocode 8. Depending on the Vs30 value, soil is classified into types A-E. The soil type is subsequently used to define a soil factor, S, which accounts for the influence of local ground conditions on seismic action. The soil factor is applied as a multiplier to the design elastic response spectrum, thereby modifying the response values. It is unity for soil type A and generally increases with smaller Vs30 values, except for soil type C, where it is slightly smaller than for soil type B. In the Bulgarian National Annex (БДС EN 1998-1:2005/NA, 2012), there is another peculiar feature, the reasons for which are not entirely known: the values of the soil coefficient for soil types D and E are 1 and 1.2, respectively, which are much lower than the recommended values in Eurocode 8, 1.35 and 1.40, respectively. Also dependent upon the soil types (and indirectly upon Vs30) are the spectral periods used to define the shape of the response spectra - TB, TC, and TD.

At any rate, whenever possible, practicable, and feasible, more advanced methods, such as seismic microzonation maps, site response analyses, etc., should be used to establish the soil factor. In research carried out by the authors (Oynakov et al., 2024a), amplification factors of up to 1.70 and 1.55 were computed for 95-year and 475-year return period events, with PGA at the bedrock level of 0.10g and 0.36g, respectively. These results were obtained from an equivalent-linear site response analysis using a single time history. Therefore, it may be expected that even higher amplification factors are possible if a large suite of time histories is analyzed. Nonetheless, the results of this study, computed from data collected at 107 borehole locations in the Sofia Basin, were compiled into tentative microzonation maps for PGA, PGV, and PGD at 95-year and 475-year return periods.

This study aims to conceptualize a general framework for developing a proxy Vs30 map for the Sofia Basin. It adopts a conceptual and methodological approach, proposing integration of available geological data, topographic DEM, and microseismic noise measurements near geological boreholes. A Vs30 proxy map for the southeastern part of the Sofia Basin, prepared using HVSR and borehole data, is presented and compared with previously published maps. A comparison of Vs30 values from available maps for a real borehole in the Lozenets district is made. The proposed framework offers improvements to previously prepared maps for the Sofia Basin by supplementing data from additional sources and by including real Vs30 measurements near geological boreholes.

STATE OF THE ART IN BRIEF

Methods for determination of Vs30

The Vs30 parameter is mainly determined using invasive geophysical methods that require drilling and provide high-accuracy measurements at depth. Among the most common of these are downhole logging and crosshole seismic logging. Alternatively, non-invasive surface-wave methods offer a faster, more economical solution for large areas. These approaches, including spectral analysis of surface waves (SASW) and multi-channel analysis of surface waves (MASW), analyze the dispersion of Rayleigh waves to model the velocity profile. Table 1 summarises the key advantages and main

limitations of both types of methods. Wair et al. (2012) provided guidelines for estimating the shear wave velocity profiles in the absence of site-specific shear wave velocity data. The authors summarized relationships between Vs30 and various geotechnical parameters, and suggested a new method for extrapolating data to 30 meters depth in the absence of sufficient information about the earth's layers. The strongest approach to compile a Vs30 map for a given territory is to integrate multiple measurement types, prioritize direct and surface-wave data (fusing borehole and surface-wave measurements with microtremor constraints), and use modern mixed-effects extrapolation models to fill gaps, producing a map that is both physically constrained and statistically robust (McPhillips et al., 2020; Weatherill et al., 2023).

Table 1. Geophysical methods for determination of Vs30

Approach	Specific Methods	Primary Data Measured	Key Advantages	Major Limitations / Constraints
In-Situ Invasive (Borehole)	Cross-hole, Down-hole, P-S Suspension Logging	Direct wave travel times or interval velocities at specific depths	Highly accurate; provides detailed, site-specific vertical velocity profiles	High cost; requires borehole drilling; localized invasive footprint
In-Situ Non-Invasive (Surface Geophysics)	MASW (Active), MAM/SPAC (Passive) arrays, ReMi, SASW, single-station HVSR	Surface-wave dispersion and/or resonance frequency information	Cost-effective; non-destructive; covers a larger lateral area than boreholes	Requires complex mathematical inversion; resolution decreases with depth
Laboratory Testing	Resonant Column, Cyclic Triaxial Torsional Shear	Shear modulus (G) and damping ratio on core samples under cyclic loads	Controls stress states and strain amplitudes precisely	Disturbance during sampling alters in-situ state; expensive.
Proxy / Empirical Relationships	Geomorphic/Topographic slope, Geological units, CPT/SPT correlations	Existing maps, digital elevation models, or standard penetration blow counts (N)	Zero to ultra-low cost; instantly available for regional scale mapping	High uncertainty; cannot replace site-specific testing for critical structures

Determination of Vs30 by proxy-based methods

Proxy-based Vs30 methods estimate time-averaged shear-wave velocity in the upper 30 m without full geophysical profiling, using variables that are easier to map regionally (e.g., slope, geology, terrain). Recent advancements have shifted from single proxies to hybrid, statistically optimized, and uncertainty-aware frameworks (Yong, 2016). These models can be classified into global and local categories. Global models, such as those by Wald and Allen (2007) and Allen and Wald (2009), use widely available proxies and diverse datasets. Heath et al. (2020) created a global Vs30 mosaic incorporating slope-based models and regional maps, though their performance declines in flat plains and sedimentary basins. Local models are area-specific and use proxies like surface geology and geotechnical data. For instance, Wu et al. (2020) compared various proxies for Sichuan Province and found that geology-based models offer better predictions based on stratigraphic age and lithology.

Recent studies highlight the benefit of combining surface geology and slope gradient for accurate Vs30 mapping, particularly in sedimentary basins. Hybrid approaches have been implemented in regions such as Italy (Gironelli et al., 2024), Greece (Stewart et al., 2014), New Zealand (Foster et al., 2019), West Bohemia (Mazanec et al., 2024), Pakistan (Ahmed et al., 2024), Spain (Navarro et al., 2025), US (McPhillips et al., 2020), and at European scale (Weatherill et al., 2023), enhancing model performance while managing complexity and calibration requirements. Gilder et al. (2022) proposed a geostatistical framework for estimating Vs30 in data-scarce areas, such as Kathmandu Valley, using proxies and sparse measurements. Hayashida et al. (2023) and Saqlain et al. (2022) demonstrated that empirical formulas and fast proxy methods, respectively, can yield accurate Vs30 estimates using microtremor data and Rayleigh-wave phase velocities.

These dispersion- and noise-based "fast" Vs30 proxy methods show operational efficiency by avoiding full inversion and are less analyst-dependent; they are suitable for rapid site characterization and physical-based methods. However, they require field measurements and array setups; performance depends on noise conditions, array geometry, and site complexity. Table 2 shows comparative data and trends in the development of Vs30 proxy maps.

Table 2. Compilation of Vs30 proxy maps applying different approaches

Single vs multi-proxy		**Deterministic vs probabilistic**	**Mapped proxies vs measurement-based proxies**	
Single proxies (slope or geology alone)	Multi-proxy and hybrid models (slope + geology + terrain + measurements)	Deterministic maps (regression-based)	Mapped proxies (slope, geology, terrain)	Measurement-based fast proxies (SPAC /CCA coefficients, VR36/VR40)
Useful for broad-scale, first-order mapping but often shows systematic biases in plains, basins, or complex geology	consistently reduce residuals and improve regional applicability, as shown in Sichuan, Marche, Muzaffarabad, and global USGS work	dominate operational use, but geostatistical/Bayesian frameworks are gaining traction because they provide uncertainty estimates essential for risk-informed design and hazard assessment	excel at regional coverage and rapid deployment	bridge the gap between full Vs profiling and purely mapped proxies, offering rapid yet physically grounded Vs30 estimates at specific sites
Wald and Allen, 2007	Ahmed et al., 2024 Gironelli et al., 2024 Heath et al., 2020 Wu et al. 2020	Gilder et al., 2022	Yong, 2016	Yong, 2016 Saqlain et al., 2022

MATERIALS AND METHODS

Geological Setting of the Sofia Basin

The Sofia Basin in western Bulgaria is a complex intramontane depression within the Sofia Graben, shaped by Neogene and Quaternary extensional tectonics (Kamenov and Kojumdjieva, 1983; Oynakov et al., 2024a). It is bounded by the active Vitosha, Lyulinsky, Lozensky, and Iskar fault systems, which created a mosaic of sub-basins with diverse depths and sedimentation through differential subsidence (Bonchev, 1971).

Tectonic segmentation causes sharp lateral variations in sediment thickness that do not align with the surface topography (Angelova, 1999; Zagorchev, 2001). Thick sedimentary packages can sit next to steep bedrock blocks, while gentle slopes may overlie shallow bedrock. This mismatch complicates the assessment of shear-wave velocity Vs30. Ongoing deformation continues to affect drainage, sediment supply, and geomorphological surfaces.

Geologically, the basin consists of heterogeneous Quaternary sediments overlying Neogene and pre-Neogene basement rocks (Yaneva et al., 2002). The Quaternary fill contains alluvial, colluvial, lacustrine, and fluvial-terrace deposits ranging from coarse gravels to fine clays. These deposits exhibit strong lateral facies transitions driven by tectonics, sediment influx, and geomorphological processes (Donkova, 2015). Mountain-derived alluvial fans feature coarse, poorly sorted gravels that transition into fine central and eastern lacustrine deposits. Sediment thickness varies significantly, exceeding 200 meters in some sub-basins while remaining under 20 meters in others (Yaneva and Donkova, 2017).

Alluvial fans originating from the Vitosha, Lyulin, and Stara Planina Mountains form prominent deposits along the basin margins. These alluvial fans consist of coarse, poorly sorted gravels and sands that coalesce down the basin into finer alluvial and lacustrine sediments. Thick sequences of fine-grained lacustrine deposits are common in the central and eastern parts of the basin, reflecting periods of reduced drainage efficiency and localized lake formation. The depth to bedrock varies considerably, with borehole data indicating sediment thicknesses exceeding 200 m in some subbasins, while other areas indicate shallow bedrock at depths below 20 m (Yaneva and Donkova, 2017).

These geological units exhibit distinct engineering-geological properties, resulting in high spatial variability in Vs30 (Ivanov, 2002). Coarse alluvial cones yield higher Vs30 values, whereas fine lacustrine and thick alluvial deposits show lower values. Consequently, detailed geological data is crucial for accurate Vs30 mapping.

The basin's geomorphology features broad alluvial plains, undulating surfaces, and incised river valleys alongside steep mountain foothills (Donkova and Radulov, 2017). While global Vs30 models rely heavily on topographic slope, this metric is unreliable in the Sofia Basin. Because of tectonic control, steep slopes can overlie both shallow and deep sediment, while flat areas can mask either thick lacustrine deposits or shallow bedrock. This weak correlation undermines slope-based Vs30 predictions and demands nuanced geomorphological analysis.

Terrain metrics derived from DEMs, such as curvature and local relief, provide additional information about depositional environments and geomorphological processes (e.g., Allen and Wald, 2009; Stewart et al., 2014). However, these metrics need to be interpreted in the broader tectonic and geological context to avoid misclassification of stratigraphical layers at

depth. For this reason, geomorphological information is included in the Vs30 assessment framework as a secondary modifier rather than a primary determinant.

General workflow to generate a proxy Vs30 map

This study proposes a methodological framework to integrate multiple datasets and constrain the geological, geomorphological, and subsurface characteristics of the Sofia Basin to generate a proxy Vs30 map. These datasets include topographic information, geological maps, borehole records, and newly performed HVSR measurements. Each dataset contributes unique and complementary information, and their combined use enhances the robustness of the Vs30 proxy model. This section describes the origin, characteristics, and preprocessing of each dataset that needs spatial harmonization and resolution adjustment. The consequence stages with separate processing steps to generate the Vs30 proxy map are as follows:

1. Initial Step: HVSR & Borehole Point Data Collection and Processing
- *Field surveying*: Conducting single-station HVSR measurements near geological boreholes.
- *Process HVSR data*: Extract single-station resonance frequencies (f_0, A_0).
- *Invert frequencies*: Perform joint inversion by higher-mode constraints using geological soil thicknesses.
- *Calculate borehole profiles*: Compute direct time-average Vs30 profiles from layer depths.
- *Integrate point data*: Cross-calibrate and combine both datasets into a unified point dataset.

The initial step of HVSR and Borehole Point Data Processing transforms raw, localized geophysical and geotechnical measurements into uniform, Vs30 point coordinates, considered as true-measured. HVSR method provides f_0 and information on impedance contrast; Vs30 is inferred through constrained inversion and/or lithology-based assumptions. This stage creates the foundational training dataset required for the spatial regression model.

2. Spatial Covariate Preparation
- *Derive terrain proxies*: Calculate slope, gradient, and Topography Roughness Index (TRI) from a 90 m DEM.
- *Resample topography*: Transform and resample data to a 100 m grid.
- *Classify geology*: Digitize rock units and sediments into categorical lithofacies.
- *Rasterize geolo*gy: Convert lithofacies maps into a matching 100 m grid.

3. Spatial Intersect & Regression Modeling
- *Extract point values*: Intersect the continuous grids at exact borehole/HVSR coordinates.
- *Train models*: Multivariate regression or Random Forests.
- *Define target function*: Model Vs30 as a function of slope, TRI, and geology.

4. Mapping the Deterministic Trend
- *Apply equations*: Run the trained regression model over the full 100 m grid.
- *Generate trend grid*: Output a long-wavelength deterministic trend map.

5. Residual Calculation & Kriging
- *Compute point residuals*: Subtract predicted Vs30 from the true-measured values.
- *Create residual list*: Compile the point-specific model errors.
- *Interpolate variations*: Perform Ordinary Kriging purely on the point residuals.
- *Generate short-wavelength grid*: Output the localized variation map.

6. Additive Merge & Validation
- *Merge rasters*: Add the trend grid to the residual raster grid.
- *Create final map*: Finalize the integrated proxy Vs30 map and grid.
- *Compile available archives*: Gather existing geotechnical reports and published maps.
- *Conduct comparative analyses*: Consistency check of results and determine differences/inferences.

Based on existing and newly acquired data, we present preliminary results from some steps of the general workflow for compiling a proxy Vs30 map described above. These results cover individual workflows from stages 1, 2, and 6.

Datasets

Topographic data

Calculating Vs30 from DEM slope is a commonly used, low-cost "proxy" method for regional seismic hazard assessment (Allen and Wald, 2009). However, it is not representative of actual local shear-wave velocities because it relies on a simplistic, statistical correlation rather than direct measurement of subsurface material stiffness (Lemoine et al., 2012).

Stewart et al. (2014) produced geologic and terrain-based site condition maps for California using geological information and 1-, 3-, 9-, and 30-arcsec DEMs. They concluded from comparative studies that the 3-arcsec data are sufficiently accurate for Vs30 determination. The choice of a 100 m resolution reflects a balance between the need to reduce noise and improve model stability, the spatial density of available geological and geophysical data, and the scale of tectonic and geomorphological features associated with Vs30, as mentioned by Gilder et al. (2022). Given these considerations, a 100 m grid was adopted for subsequent analysis. Slope was computed using standard GIS algorithms. The topographic slope value for each grid cell was calculated using nearest-neighbor interpolation, and the TRI was calculated as the square root of the sum of the squared differences between the elevation of a central cell and its 8 surrounding neighbor cells (Zevenbergen and Thorne, 1987; Riley et al., 1999).

Geological Drilling

Borehole and geological data have been collected from the literature to complement the indirect Vs measurements. In this study, we used Vs30 data inferred from 68 boreholes in the southeastern part of the Sofia basin, published by Ilieva et al. (2003). The inferred velocity field along the north-to-south and west-to-east profiles crossing the basin varied in both vertical and lateral directions. In the near-surface part of the boreholes, the horizontal seismic wave velocity layer has not formed due to strong shear wave velocity variability, especially in the north-south direction along the profiles.

Microseismic noise measurements

The measurements were conducted over the last 3 years at 68 sites near the boreholes (see Fig. 1) in the southeastern part of the Sofia Basin, using the methodology described by Oynakov et al. (2024b). Microseismic recordings lasting 20 minutes were made with Etna2 accelerometers, with the instrument placed on natural terrain to ensure good ground contact. The data processing of HVSR microseismic records was performed using the Geopsy software (Wathelet et al., 2020), available at https://www.geopsy.org.

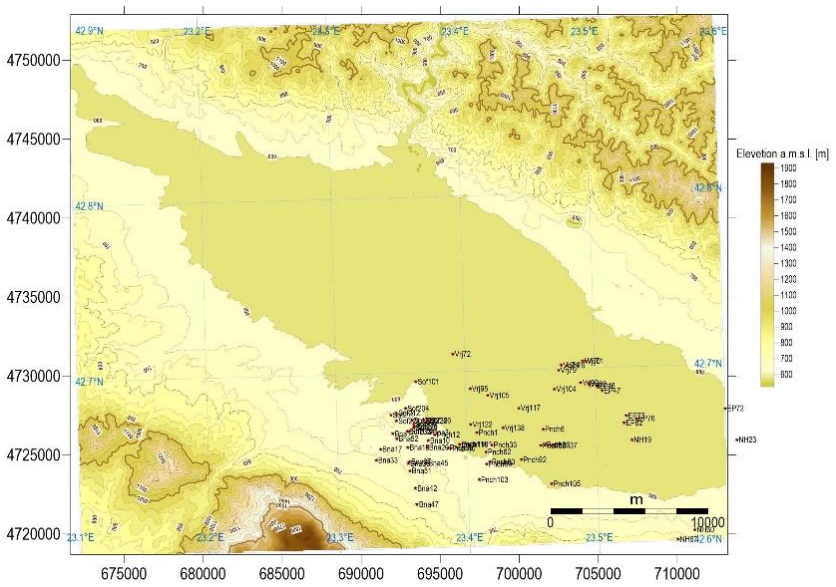


Fig. 1. Map of the measurement points (marked with a red star) in the southeastern part of the Sofia Basin. The basemap is a topography DSM model from the TANDEM-X 100 m grid in UTM 34N.

Characteristics of Available Vs30 Maps

In the Sofia region, over the last two decades, several Vs30 maps with varying spatial resolutions have been published in the scientific literature, as shown in Fig. 2a-c. They were produced using different source data and methodological approaches. A comparison of two maps—the Eurocode 8 Subsoil layer classes A, B, C, D, and E map (Fig.2a) and the Zoned Velocity Block Map (Fig.2b)—provides a detailed correlation between categorical soil classifications and their quantified shear-wave velocity Vs30 microzonation ranges for the Sofia Basin. The two maps collectively show a clear geological transition across the Sofia Basin, directly linking Eurocode 8 subsoil classes to specific shear-wave velocity Vs30 profiles. The stable mountain foothills in the south feature rock and very stiff formations (Classes A and B) characterized by the basin's highest stiffness velocities, peaking between 350 m/s and 1,420 m/s (Block 3). Moving toward the south-central and southeastern transition zones (Bojana and Gorubljane), the ground shifts to intermediate, dense sediment deposits (Class C) with mid-range velocities between 250 m/s and 680 m/s (Block 1.2). A significant difference

is noted in the Vs30 values for Block 1.2, ranging from 150 to 190 (Fig. 2b), directly in the foothills of Vitosha, compared to those in Fig. 2a. Finally, the northern plain and basin center (such as Obelja) flatten out into thick, soft-to-medium cohesive soils (Class D) and specialized alluvial anomalies (Class E), which yield the basin's lowest shear wave thresholds ranging from 160 m/s to 480 m/s (Blocks 1.3 and 2).

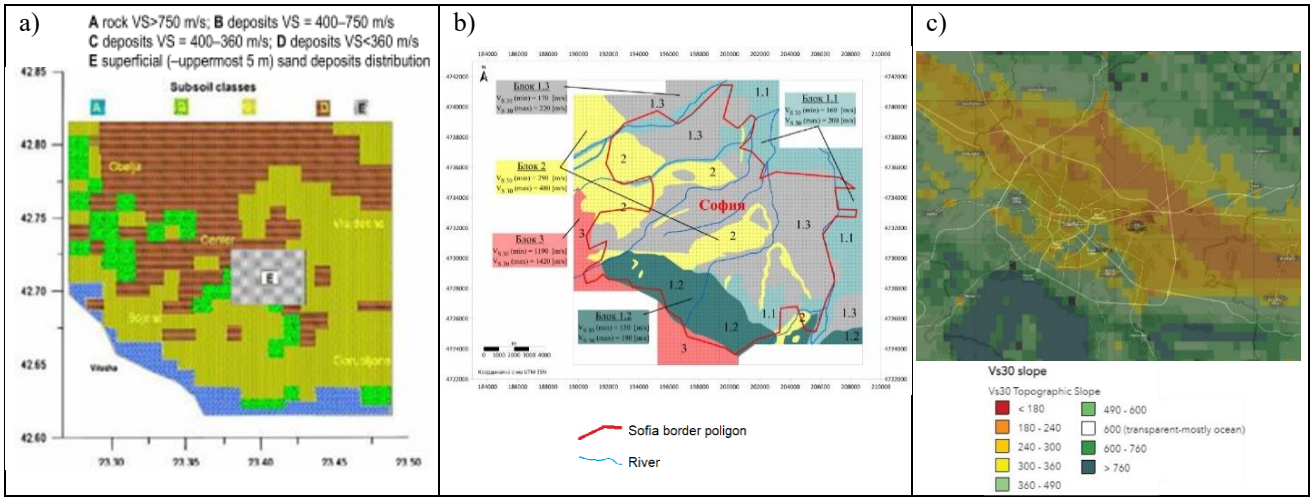


Fig. 2. Models of Vs30 parameter: a) (Dineva et al., 2008); b) min-max Vs30 (Georgieva et al., 2020); c) USGS Vs30 (https://earthquake.usgs.gov/data/vs30/).

On the other hand, the USGS Vs30 map (Allen and Wald, 2007), shown in Fig 2c, provides a global, topographic-slope-based model that differs significantly from the previous two local geological maps of the Sofia Basin in both methodology and local precision. The USGS Vs30 map has been derived from USGS slope topography. It is available on a regular grid in raster format with a resolution of 30 arc-seconds (0.00833333°), corresponding to a ~730 by ~930 m grid in longitude and latitude for the Sofia Basin (Heath et al., 2020). Several differences are noticeable between this global map and the previous two. The USGS map estimates that the central Sofia valley (orange/yellow zones) has velocities of 240–300 m/s and 180–240 m/s. In contrast, the localized map in Fig. 3b explicitly reveals softer soils (Block 1.3) with a much lower minimum threshold of 171 m/s, and the map in Fig 2a highlights highly specialized, potentially high-risk soft soils (Class E) right in the Sofia City center that the USGS slope model completely misses. The local maps show highly irregular, geologically complex soil boundaries and localized "pockets" (such as Obelja and central anomalies). The USGS map shows a highly generalized, smooth, northwest-to-southeast linear corridor, dictated solely by macro-topography, and ignores localized alluvial deposits and subsurface sedimentary variations. For the Vitosha mountain skirt (Zheleznitsa/Vladaya), the USGS map assigns a broad classification of >760 m/s (dark green). While this aligns with Eurocode 8's Class A (>800 m/s) in Fig. 2a, it lacks the precise, localized geotechnical boundaries found in Fig. 2b, which explicitly break the hard terrain into distinct velocity blocks up to 1430 m/s. The first two maps rely on direct in-situ geotechnical measurements (boreholes, seismic profiling, and Eurocode criteria). The USGS map uses a proxy-based topographic slope model that assumes a correlation between surface gradient and stiffness, thereby naturally smoothing out complex flat-basin geology, such as that of Sofia City. By underestimating the basin's softness at the center and missing localized Class E anomalies, the USGS model can significantly underpredict seismic site amplification and peak ground acceleration during an earthquake. Consequently, relying solely on the USGS topographic proxy rather than local geotechnical data may result in the dangerous underdesign of structures in Sofia's most vulnerable urban areas.

Methods

An effective local-level shear wave velocity (Vs30) scheme balances cost, spatial coverage, and accuracy by combining three distinct approaches: regional proxy mapping, non-invasive surface-wave geophysics, and invasive borehole measurements. This integrated, multi-level approach optimizes resources by using sparse, high-precision data to calibrate dense, less expensive measurements across the municipality.

Vs30 Prediction Based on Topographic Slope

After obtaining the topographic slope in the southeastern part of the Sofia Basin, each grid cell is assigned an NEHRP site category based on the active tectonic region. Based on changes in the corresponding slope in certain ranges, Vs30 was categorized for soils of types E (D according to БДС EN 1998-1:2005/NA), D (C according to БДС EN 1998-1:2005/NA), C (B according to БДС EN 1998-1:2005/NA), and A/B (according to БДС EN 1998-1:2005/NA), respectively (see Table 1). In some countries, a more detailed categorization of the different classes is adopted or

recommended (e.g., Kanlı et al., 2006; Ciancimino et al., 2018), as well as different Vs30 threshold values for site type classification (e.g., Adeel et al., 2023; Smerzini et al., 2026).

Table 1. Ranges of topographic slopes proposed by Wald and Allen (2007) and Allen and Wald (2009) for the classification of sites into NEHRP categories

NEHRP site class	Vs30 range	Equivalent EC8 class	БДС EN 1998-1:2005/NA		Slope range (m/m)	
			Ground-based type	Vs30 range	Active tectonic (Wald and Allen, 2007)	Active tectonic (Allen and Wald, 2009)
A	>1500 m/s					
B	760 – 1500 m/s	A	A	>800 m/s	>0.138	>0.14
C	360 – 760 m/s	B	B	360 – 800 m/s	0.018 – 0.138	0.018 – 0.14
D	180 – 360 m/s	C	C	180 – 360 m/s	0.0001-0.018	0.0003-0.018
E	<180 m/s	D	D	<180 m/s	<0.0001	<0.0003
F*		E/special cases	E	-		
		S_1** and S_2				

* *Soils requiring site response analysis (Source: https://www.fema.gov/sites/)*

** *<100 m/s (indicative) (Source: EC8-1; https://help.geostru.eu/loadcap/en/eurocodice8.htm)*

HVSR analysis

The microseismic noise was processed using the HV toolbox in the Geopsy environment, following the recommendations of the SESAME project (2004). For each microtremor measurement point, the signals were divided into appropriate time windows, and anti-trigger removal was applied. A H/V spectral curve was calculated, and the main resonance peak (f_0) was identified as the most stable and dominant maximum. After that, a check for secondary peaks was performed, and the curve quality was assessed. Peak amplitude A_0 was determined from the H/V curve. The approximate relation $H \approx Vs/4f_0$ was used only as a first-order consistency check between the observed resonance frequency and the expected depth to the main impedance contrast. This step provides a reliable estimate of the fundamental frequency f_0 and primary information about the impedance contrast.

A) Velocity model parameterization

The layer thicknesses are taken from real engineering-geological boreholes located near the microseismic measurement points. Thus, the model's geometry is geologically justified. The velocity model (initial Vs values by layer) is borrowed from a similar alluvial valley in California, where measured shear-wave profiles are available. This model is used as an a priori assumption and not as a ground truth. In the inversion procedure of the GEOPSY Dinver program (Wathelet et al., 2020), the layer thicknesses at the microtremor measurement points near the borehole are set to vary by ±20–30%. Vs velocities in each layer are allowed to vary by ±20–30%, the parameters Vp and density are set within realistic limits corresponding to the lithology, and the number of layers is fixed based on the drilling information. This constrained inversion approach reduces solution ambiguity and is consistent with SESAME recommendations for using geological a priori information.

B) Inversion in Dinver

In the Dinver toolbox, ellipticity inversion of Rayleigh waves was used as a proxy for HVSR, with the following settings: the ellipticity curve is enabled (main control of the shape of the curve), the ellipticity peak is enabled (fixing the resonance frequency f_0), the weight of the peak is ≈ 0.3 with respect to the curve to stabilize the solution without dominating, the criterion for model acceptance is chosen to be a minimal misfit, and analysis of an ensemble of valid models. Fixing the peak ensures that the inversion reproduces the observed fundamental resonance, which is a key parameter according to SESAME.

C) Determining Vs30 by the Dinver toolbox

From each accepted model, Vs30 was calculated using the standard formula:

$$V_{s30} = \frac{30}{\sum_{i=1}^{n} \frac{h_i}{v_{si}}}$$

Where h_i is the layer thickness and V_{si} is the shear rate in the layer.

D) Geological Vs30 profiles

A table called Vs30_BoreholesUsed (not shown here) was prepared with calculated Vs30 from the borehole stratigraphy and assumed Vs values by lithology (Oynakov et al., 2024a; b). The Vs30 calculated in the Dinver toolbox is an engineering-geological estimate independent of the microseismic inversion.

RESULTS AND DISCUSSION

Topographic data processing

For this study, we use a Digital Elevation Model (DEM) from the TanDEM-X satellite mission with a 90 m spatial resolution (Wessel, 2016; Wessel et al., 2018). The TanDEM-X 90 m data are freely available on EOC Geoservice (https://download.geoservice.dlr.de/TDM30_EDEM/; last access: April 27, 2026). It provides a high-accuracy Digital Surface Model (DSM) with absolute vertical accuracy of up to 10 m (90% confidence) and relative accuracy of 2–4 m, depending on slope (González et al., 2020). The DEM is referenced to the WGS84-G1150 ellipsoid and converted to orthometric heights using the EGM08 geoid with a 2.5' cell size, in a common datum. The DEM data were resampled to 100 by 100 m in the projected coordinate system, using WGS 84/UTM zone 34N, from which topographic parameters (slope, gradient, and TRI) are determined, as shown in Fig. 3. At this stage of the study, terrain indicators were extracted, calculating the slope, gradient, and TRI from the reassembled data for a 100 m grid. The next steps in stage 3 are to digitize geological maps and convert them to a common raster format and scale.

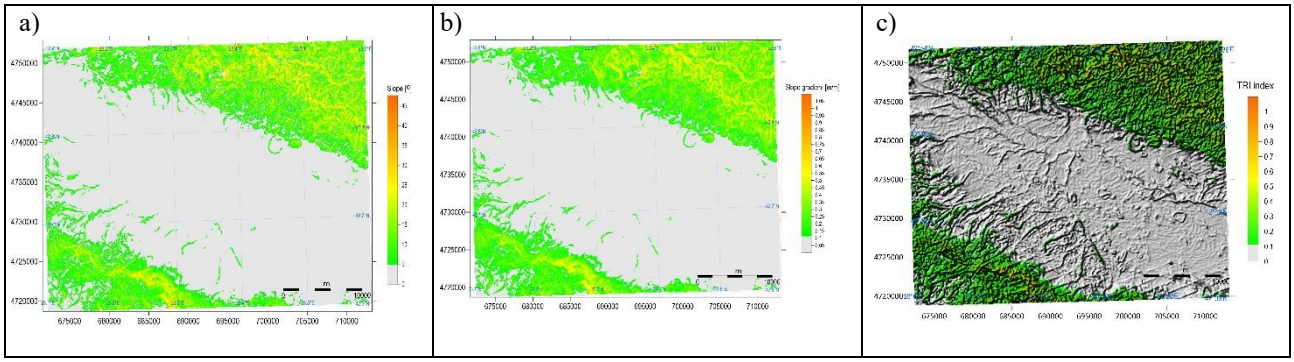


Fig. 3. Calculated topographic parameters from DEM: a) slope [°]; b) gradient [m/m]; c) TRI.

HVSR and borehole data integration

The newly compiled Vs30 model following the SESAME (2004) project recommendations is shown in Fig 4. The model is produced using Dinver + HVSR + borehole data, which uses actually measured resonant frequencies, real boreholes compiled with local velocity models, and an inversion of each HVSR-measured point separately. The HVSR analysis was primarily used to determine the fundamental resonance frequency f_0 and to assess the presence of a significant impedance contrast. Since single-station HVSR alone does not uniquely determine Vs30, the derived Vs profiles and Vs30 values should be interpreted as constrained inversion-based estimates supported by borehole stratigraphy and lithological constraints. To reduce non-uniqueness, the results need be compared with MASW/MAM/SPAC, downhole/crosshole, or CPT/SPT data where available.

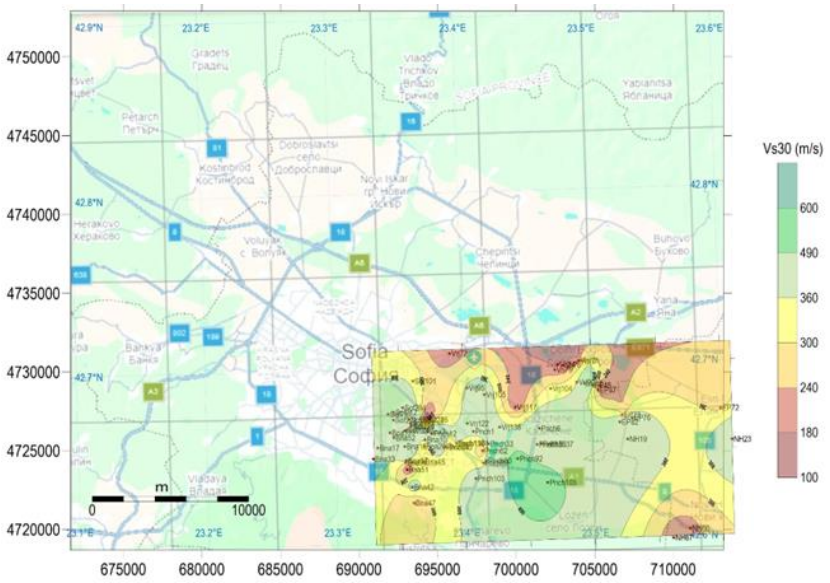


Fig. 4. Compiled Vs30 model based on the data from HVSR measurements and geological boreholes.

Vs30 values derived from the constrained Dinver inversion range from 112.4 to 527.8 m/s, with a mean of 356.6 m/s and a median of 390.5 m/s. The lithology-based Vs30 estimates range from 232 to 483 m/s. When comparing the Vs30 values calculated by the Dinver program, it is found that the values using HVSR data are lower than those from the geological boreholes at 42 locations, which vary from 0 to 184 m/sec, and for the rest, the values of Vs30 from the geological boreholes exceed those from the calculated ones, varying from 0 to 305 m/sec.
The comparison between the Vs30 from the Dinver toolbox and the geological Vs30 shows three main groups of results:

- A good agreement between the two approaches is observed when the difference is < 15% (small differences) for some points. This result shows that the HVSR peak correctly reflects the depth and impedance contrast, the velocity model is realistic, and the parameterization is stable.
- HVSR's sensitivity to deeper contrasts can explain moderate differences of 15–30%, the ambiguity of the inversion, or variations in Vs in the upper 30 m, which HVSR does not always directly control.
- Significant differences (>40%) are obtained at some points. Dinver gives values that are significantly lower or higher than the geological Vs30.

Agreement within ±15% is observed at 37 points, moderate discrepancy of 15–30% at 19 points, and discrepancy exceeding 40% at 12 points. Possible explanations for these differences could be that the HVSR is dominated by deeper contrast rather than the shallow 30 m, that local variations in lithology are not well accounted for in the velocity model borrowed from California (Radulov, personal communication), or that the equivalent solutions are non-unique. It is important to emphasize that the HVSR method is most sensitive to the resonant frequency and impedance contrast, but does not always provide an unambiguous determination of Vs30. Therefore, in the next analyses, local data from Ilieva et al. (2003), engineering-geological profiles, and additional information, where available, will be used.

Based on the analysis performed, we can conclude that there are no indications of methodological error in the HVSR processing; the inversion is geologically constrained (not a free inversion), the peak fixation is applied correctly; the ±20–30% variation is within reasonable limits, and the discrepancies are the result of physical ambiguity, not procedural error. This preliminary study constrained the HVSR/proxy Vs30 model to achieve better resolution in the calibrated SE basin, especially near the borehole/HVSR control points. The model can reveal sedimentary heterogeneity that slope-only models tend to smooth out. Reliability should be expressed as confidence intervals and preliminary consistency-check errors, not as a single qualitative label. The results also reveal that surface morphology alone is insufficient for Vs30 mapping in sedimentary basins; the southeastern Sofia Basin shows stronger near-surface heterogeneity than a slope-only proxy would suggest. Combining ambient-noise resonance information with borehole/lithological constraints improves the physical plausibility of the Vs30 model. The applied HVSR inversion using the Dinver tool is non-unique and should be combined with MASW/MAM arrays, a lithology-based Vs30 estimate, or CPT/SPT correlations, where available.

Comparison of results with other Vs30 maps

Comparing the Vs30 maps obtained from HVSR and borehole data reveals similarities and differences in the Vs30 maps shown in Fig. 2. In Fig. 2a, the Vs30 map of the Sofia Basin by Dineva et al. (2008) is divided into Eurocode soil classes, as the central Sofia is mainly class D (<360 m/s), the eastern parts move to classes C and B, and at the foothills of Vitosha are class A or B. The area around the Sofia airport is mainly class D–C. These results match the newly compiled HVSR + borehole map surprisingly well. The central part around the Bulgarian National Army (BNA), National Palace of Culture, Krasno Selo, and the Medical Academy is 150–300 m/s; eastward to Mladost and Gorublyane, Vs30 gradually increases to 300–500 m/s; northeastward, sections >500 m/s appear, which practically reproduces the spatial trend of Fig. 2a' map.

The map by Dineva et al. (2008) is based on a limited set of borehole and engineering-geological data and therefore represents a generalized approximation of the subsurface conditions in Sofia.

The new Vs30 map is compiled from dozens of HVSR points and local boreholes and shows smooth transitions between zones. The newly compiled Vs30 map has a higher spatial resolution. Comparison with USGS slope-based Vs30 (Fig. 2c) shows greater differences. For the Sofia Basin, using only topographic slope to generate a Vs30 map is problematic because the basin is almost flat, sediment thickness varies greatly, and the slope does not reflect the depth to bedrock, as shown in Fig. 3. The USGS Vs30 map shows large areas with 240–360 m/s, relatively smooth variations, and a lack of local anomalies. On the Vs30 map shown in Fig. 3, local soft zones around the BNA, the transitions to Pancharevo, local hard bodies, and sedimentary depressions are shown. These features are missing in the USGS Vs30 slope-based model.

The spatial distribution of Vs30 derived from HVSR inversion and constrained by local borehole information is broadly consistent with the main geotechnical zones proposed by Dineva et al. (2008), while indicating substantially greater spatial variability within the Sofia Basin. In contrast to the slope-based USGS Vs30 models, the HVSR-derived model appears to capture finer-scale sedimentary structures and impedance contrasts within the basin interior.

The Dinver inversion program tool is performed as a constrained problem with realistic boundaries. For some points, a good match is observed between the Dinver Vs30 and the geological Vs30. At other points, significant differences are observed due to the HVSR's limited sensitivity to the upper 30 m and the ambiguity of the inversion. The Dinver Vs30 should be interpreted in the context of the geological information and the quality of the H/V curve. While the first results provide the efficacy of the integrated point dataset, several remaining phases of the proposed workflow must be executed to compile a comprehensive, field-ready microzonation map. Immediate future efforts will focus on completing the spatial covariate preparation, which includes digitizing and lithofacies-classifying the regional geological maps into a matching 100-meter raster grid

CONCLUSION AND FURTHER WORK

This study establishes a robust, geologically constrained framework for constructing a high-resolution hybrid Vs30 proxy map of the southeastern Sofia Basin. The preliminary findings confirm that standard global models, which rely strictly on macroscopic topographic slope as a proxy for shear-wave velocity, are inadequate for the complex intramontane setting of Sofia. By neglecting localized alluvial deposits, thick lacustrine basins, and hidden bedrock steps, pure terrain models risk underpredicting seismic site amplification and peak ground acceleration in densely populated urban centers.

By integrating localized borehole data with cost-effective, non-invasive HVSR microseismic noise recordings, this research bridges the gap between sparse, high-precision direct measurements and broad spatial models. The resulting Vs30 distribution inferred following the SESAME (2004) methodological recommendations successfully captures the intense spatial heterogeneity and localized sedimentary variations inherent to the southeastern part of the Sofia Basin. The multi-level approach demonstrates that locally calibrated geophysical data are indispensable for establishing reliable site-effect multipliers, ensuring compliance with building codes, and preventing structural underdesign of critical civil infrastructure. While the first results compare the efficacy of the integrated point dataset, several remaining phases of the proposed workflow must be executed to compile a comprehensive, field-ready microzonation map. Immediate future efforts will focus on completing the spatial covariate preparation, which includes digitizing and lithofacies-classifying the regional geological maps into a matching 100-meter raster grid.

Following dataset alignment, advanced multivariate regression models and machine-learning frameworks, such as Random Forests, will be trained to establish the broad, deterministic long-wavelength trend of the basin's Vs30 distribution. To account for localized residuals and short-wavelength variations, Ordinary Kriging will be applied to the point-specific model errors. An additive merge of the deterministic trend and interpolated residual maps will then be validated against independent engineering-geological archives. Future investigations will address the non-uniqueness and moderate discrepancies (15–30%) observed between the Dinver numerical inversions and true geological layer depths. Multi-station microtremor arrays can be incorporated better to constrain shear-wave variations within the uppermost shallow sediment layer. Next steps include extending ambient-noise and/or surface-wave measurements to the western Sofia Basin and integrating all data into a single calibrated model. Expanding this synchronized workflow across the entire Sofia Basin will provide the definitive geophysical foundation needed for resilient urban planning and definitive seismic microzonation.

Acknowledgements
The work presented was carried out within the project Assessment of Earthquake Ground Motion Amplification in the Sofia Basin, funded by the Bulgarian National Science Fund, contract number КП-06-Н64/1, effective from 15.12.2022.

REFERENCES

Adeel, M. B., Nizamani, Z. A., Aaqib, M., Khan, S., Rehman, J. U., Bhusal, B., & Park, D. (2023). Estimation of VS30 using shallow depth time-averaged shear wave velocity of Rawalpindi–Islamabad, Pakistan. Geomatics, Natural Hazards and Risk, 14(1), 1–21. https://doi.org/10.1080/19475705.2022.2161953

Ahmed, T., Rehman, K., Shafique, M. et al. (2024). Proxy-based Vs30 modelling of the Muzaffarabad, northern Pakistan. Environ Earth Sci 83, 188, https://doi.org/10.1007/s12665-024-11502-8

Allen, T. I., Wald, D. J. (2009). On the use of high-resolution topographic data as a proxy for seismic site conditions (Vs30). BSSA, 99(2A), 935–943.

Angelova, D. (1999). Neotectonic structures and their dynamics in the Sofia complex graben, Bulgaria, In: Proceedings of 2nd Balkan Geophysical Congress and Exhibition, 5-9 July 1999, Istanbul, Turkey, 280-281.

Bonchev, E. (1971). Problems of Bulgarian Tectonics. Sofia, Technika Pbl House, 204 p. (in Bulgarian).

БДС EN 1998-1:2005/NA (2012). BSI EN 1998-1/NA Eurocode 8: Design of structures for earthquake resistance – Part 1: General rules, seismic actions and rules for buildings, National Annex for Bulgaria, https://bds-bg.org/images/upload/Nacionalni_prilojenia/BDS_EN_1998-1_NA.pdf.

Ciancimino, A., Foti, S., Lanzo, G. (2018). Stochastic analysis of seismic ground response for site classification methods verification, Soil Dynamics and Earthquake Engineering, 111, 169-183, https://doi.org/10.1016/j.soildyn.2018.04.006.

Dineva, P., Paskaleva, I., La Mura, C., Panza, G. (2008). Hybrid MS-BIEM for Seismic Site-Response Phenomena: A Case Study of Sofia. In: Zaicenco, A., Craifaleanu, I., Paskaleva, I. (eds) Harmonization of Seismic Hazard in Vrancea Zone. NATO Science for Peace and Security Series C: Environmental Security. Springer, Dordrecht. https://doi.org/10.1007/978-1-4020-9242-8_10

Donkova, Y. (2015). Sedimentological characteristics of Quaternary sediments in the southern board of the Sofia Basin. Proceedings of the National Conference "GEOSCIENCES 2015", Bulgarian Geological Society, Sofia, 109-110.

Donkova Y., Radulov A. (2017). Morphology of two normal-fault scarps along the North Sofia fault: traces from repeating earthquakes. National conference "Geosciences 2017" with international participation, Bulgarian Geological Society, Sofia, pp. 111–112. (in Bulgarian).

EN-1998-1 (2005) Eurocode 8, Design of Structures for Earthquake Resistance, Part 1: General Rules, Seismic Actions and Rules for Buildings. European Committee for Standardization, CEN, 36 B-1050, Brussels.

Foster, K. M., B. A. Bradley, C. R. McGann, and L. M. Wotherspoon. 2019. "A VS30 Map for New Zealand Based on Geologic and Terrain Proxy Variables and Field Measurements." Earthquake Spectra 35, no. 4: 1865–1897. https://doi.org/10.1193/121118EQS281M.

Georgieva, B., Ranguelov, B., Solakov, D., Dimovsky, S., Kisyov, A. (2020). Methodology of mapping and digitalization of Vs30 for the seismic hazard assessment in big cities, Journal of Mining and Geological Sciences, 63, 210-2013.

Gilder, C. E. L., De Risi, R., De Luca, F., Pkhrel, R., Vardanega, P. J. (2022). Geostatistical framework for estimation of VS30 in data-scarce regions. BSSA, 112(6), 2981–3000, https://doi.org/10.1785/0120210266

Gironelli, V., Volatili, T., Luzi, L., Brunelli, G., Tondi, E. (2024). Dual-proxy estimation of Vs30: the case study of the Marche Region (central Italy), Journal of Maps, 20:1, 2349787, DOI: 10.1080/17445647.2024.2349787

González, C., Bachmann, M., Bueso-Bello, J.-L., Rizzoli, P., Zink, M. (2020) A Fully Automatic Algorithm for Editing the TanDEM-X Global DEM. Remote Sensing 12(23): 3961. https://doi.org/10.3390/rs12233961

Heath, D., Wald, D. J., Worden, C. B., Thompson, E. M., Scmocyk, G. (2020). A Global Hybrid VS30 Map with a Topographic-Slope-Based Default and Regional Map Insets", Earthquake Spectra, vol. 36, 3: pp. 1570-1584.

Ilieva M., Slavov S., Gavrilova G., Tzvetanova V. (2003). Vertical velocity sections in the near-surface part of the Sofia graben, Geologica Balcanica, 33(1-2): 75-93, DOI: 10.52321/GeolBalc.33.1-2.75.

Ivanov, P. (2002). Engineering geological conditions in the Sofia kettle and consequences from the earthquakes. – Geologica Balc., 32, 2–4, 117–122. DOI: 10.52321/GeolBalc.32.2-4.117

Kanlı, A.I., Tildy, P., Prónay, Z., Pınar, A., Hermann, L. (2006) VS30 mapping and soil classification for seismic site effect evaluation in Dinar region, SW Turkey, Geophysical Journal International, 165(1), 223–235, https://doi.org/10.1111/j.1365-246X.2006.02882.x

Kamenov, B., Kojumdgieva, E. (1983). Stratigraphy of the Neogene in the Sofia basin, Palaeontology, Stratigraphy and Lithology 18, 69–85 (in Bulgarian, with English abstract).

Lemoine, A.; Douglas, J.; Cotton, F. (2012). Testing the Applicability of Correlations between Topographic Slope and VS30 for Europe. Bulletin of the Seismological Society of America, 102(6), 2585–2599, https://doi.org/10.1785/0120110240

Mazanec, M., Valenta, J., Málek, J. (2024). Does VS30 reflect seismic amplification? Observations from the West Bohemia Seismic Network. Nat Hazards 120, 12181–12202, https://doi.org/10.1007/s11069-024-06679-x.

McPhillips, D.F., Herrick, J.A., Ahdi, S., Yong, A.K., and Haefner, S. (2020). Updated Compilation of VS30 Data for the United States: US Geological Survey data release, https://doi.org/10.5066/P9H5QEAC.

Navarro, M., L´opez, F., Martínez-Pag´, an P., García-Jerez, A., Martínez-Segura, M.A., Oda, Y., Enomoto, T.(2025). Estimating Vs30 structure from topographic and geological data in the southeast of Spain. Eng Geol., 351:108037. https://doi.org/10.1016/j.enggeo.2025.108037.

Oynakov, E., Ivanov, R., Radulov, A., Pashova, L., Popova, M., Donkova, Y. (2024a). Equivalent linear site response analysis for the Sofia Basin, In: Proceedings of 18th World Conference on Earthquake Engineering (WCEE2024), June 30 – July 5 2024, Milan, Italy, https://proceedings-wcee.org/view.html?id=25269&conference=18WCEE

Oynakov, E.; Ivanov, R.; Dimitrova, L.; Radulov, A (2024b). Evaluation and analysis of microseismic records on the territory of the Sofia basin. J. Theor. Appl. Mech., 54, 429–445, doi: https://doi.org/10.55787/jtams.24.54.4.429

Riley, S. J., DeGloria, S. D., & Elliot, R. (1999). A Terrain Ruggedness Index That Quantifies Topographic Heterogeneity. USDA Forest Service, Proceedings: Rocky Mountain Research Station, Intermountain Journal of Sciences, 5 (1-4), 23-27.

Saqlain, M., Zada, U., Muhammad, G., AlQahtani, S. A., Ali, Z., Hussain, W. (2022). Assessment of a Fast Proxy of Vs30 (Vs30m). Sustainability, 14(20), 13668. https://doi.org/10.3390/su142013668.

Smerzini, C., Paolucci, R., Sgobba, S., Ramadan, F (2026) Vertical Seismic Action for Design: Developments for the Next Generation of European and Italian Norms. Earthquake Engineering & Structural Dynamics55, 2, 350–362. https://doi.org/10.1002/eqe.70086

Stewart, J. P., Klimis, N., Savvaidis, A., Theodoulidis, N., Zargli, E., Athanasopoulos, G., Pelekis, P., Mylonakis, G., Margaris, B. (2014).Compilation of a local Vs profile database and its application for inference of Vs30 from geologic- and terrain-based proxies. Bulletin of the Seismological Society of America, 104(6), 2827-2841, https://doi.org/10.1785/0120130331

TDM90_DEM (2023) TanDEM-X - Digital Elevation Model - Global, 90m, DLR/EOC, DOI: 10.15489/ju28hc7pui09, https://geoservice.dlr.de/web/datasets/tdm90_dem

Weatherill, G., Crowley, H., Roullé, A. et al. (2023). Modelling site response at regional scale for the 2020 European Seismic Risk Model (ESRM20). Bull Earthquake Eng 21, 665–714, https://doi.org/10.1007/s10518-022-01526-5

Wair, B. R., DeJong, J. T., & Shantz, T. (2012). Guidelines for Estimation of Shear Wave Velocity, PEER Report 2012-08. Pacific Earthquake Engineering Research Center, University of California, Berkeley, CA.

Wald, D. J., Allen, T. I. (2007). Topographic slope as a proxy for seismic site conditions and amplification. BSSA, 97(5), 1379–1395.

Wathelet, M. Chatelain, J.-L., Cornou, C., Di Giulio, G., Guillier, B., Ohrnberger, M., Savvaidis, M. (2020). Geopsy: A User-Friendly Open-Source Tool Set for Ambient Vibration Processing, Seismological Research Letters, 91(3) 1878-1889, https://doi.org/10.1785/0220190360.

Wessel, B. (2016) TanDEM-X Ground Segment – DEM Products Specification Document. EOC, DLR, Oberpfaffenhofen, Germany, Public Document TD-GS-PS-0021, Issue 3.1, https://tandemx-science.dlr.de

Wessel, B., Huber, M., Wohlfart, C., Marschalk, U., Kosmann, D., Roth, A. (2018). Accuracy assessment of the global TanDEM-X Digital Elevation Model with GPS data. ISPRS Journal of Photogrammetry and Remote Sensing 139: 171–182. https://doi.org/10.1016/j.isprsjprs.2018.02.017

Wu, W., Liu, J., Guo, L. et al.(2020). Methodology and Assessment of Proxy-Based Vs30 Estimation in Sichuan Province, China. Int J Disaster Risk Sci 11, 133–144, https://doi.org/10.1007/s13753-020-00253-2

Yaneva, M., Berov, B., Frangov, G. (2002). Evolution of Sofia Basin during the Neogene. Geologica Balkanica, 32, 135-138, DOI: 10.52321/GeolBalc.32.2-4.135

Yaneva, M., Donkova, Y. (2017) Quaternary deposits of the alluvial rivers in Sofia Basin. Comptes rendus de l'Académie bulgare des Sciences,70, 1, 103-110.

Yong, A. K. (2016). Comparison of measurement- and proxy-based Vs30 values in California. Earthquake Spectra, 32(1), 171–192, https://doi.org/10.1193/013114EQS025M

Zagorchev, I. (2001) Introduction to the geology of SW Bulgaria, Geologica Balcanica, 31, 1-2, 3-52, https://geologica-balcanica.eu/journal/31/1-2/pp.-3-52

Zevenbergen, L. W., Thorne, C. R. (1987). "Quantitative Analysis of Land Surface Topography." Earth Surface Processes and Landforms, 12(1), 47-56. https://doi.org/10.1002/esp.3290120107

BIOGRAPHY

Lyubka Pashova is an Associate Professor in the Geodesy Department at the National Institute of Geophysics, Geodesy and Geography, Bulgarian Academy of Sciences. She holds an M.Sc. degree in "Geodesy, Photogrammetry and Cartography" and a PhD in Geodesy. Her research and publications focus on statistical methods for geodetic data processing, coordinate reference systems, and geospatial information processing and analysis. She is a member of the Bulgarian Cartographic Association and the International Association of Geodesy, and of the editorial teams of the Micro, Macro & Mezzo Geo-Information and Estuarine Management and Technologies Journals. She leads and participates in several geodesy and geodynamics projects at the national and international levels. Since October 2014, she has been the GEO Principal Alternate for Bulgaria in the Group on Earth Observations.

Emil Iliev is an Associate Professor in the Department of Seismology and Seismic Engineering at the National Institute of Geophysics, Geodesy and Geography, Bulgarian Academy of Sciences. He specializes in seismology and seismic engineering. His primary research focuses on monitoring regional seismicity and evaluating spatial-temporal variations in earthquake catalogs across the Balkan region. He uses advanced statistical tools to investigate seismic precursors, tracking parameters such as b-values to understand the preparation phases of earthquakes. Additionally, his work includes conducting seismic hazard assessments and analyzing site-specific ground motions to mitigate environmental disaster risks. Through these computational modeling and monitoring efforts, he contributes significantly to regional geophysical disaster prevention platforms.

Radan Ivanov is a Professor in the Department of Seismology and Seismic Engineering at the National Institute of Geophysics, Geodesy and Geography, Bulgarian Academy of Sciences, and is the manager of the National Strong Ground Motion Network. His scientific interests are focused on seismic monitoring of strong ground motions; seismic instrumentation, monitoring and field dynamic testing of buildings, facilities and cultural monuments; processing, analysis and evaluation of strong-motion and experimental data; experimental identification of the dynamic properties of buildings and facilities; modeling and analysis of the dynamic behavior and the failure modes of buildings, facilities and equipment by the Finite Element Method and the Discrete Element Method; seismic behavior of buried pipelines.